Cume

This cume deals with the paper "CCD uvbyHβ Photometry in Clusters..." by Barbara and Bruce Twarog 2000 A.J 120,3111. Since it is rather lengthy only the first portion of the paper is attached. Portions of the attached paper have also been whited-out by me.

To receive a passing grade on this cume you must earn 70 points.

- 1. (12 pts) Define the following terms. Employ an equation in your definition when appropriate.
 - a) uvbyHß
 - b) c_1, m_1
 - c) standard error of the mean
 - d) PSF
- 2. (15 pts) Discuss the reasonableness or unreasonableness of the following uncommon statements found in this paper.
 - a. Section 2.3 Line 1 "Observations... were obtained on two nights...with the first of these two being photometric." Shouldn't the measurements on the non-photometric night have been discarded? Why or why not?
 - b. Section 2.4 line 1 "Two nights were dedicated ...with one night photometric." Shouldn't the non-photometric data have been discounted? Why or why not?
 - c. Page 3116, end of first paragraph "...completeness of the sample is irrelevant..." Generally we strive for completeness, why do the authors state it is "irrelevant" to their study?
- 3. (12 pts) Outline the procedure used to transform observed b-y into a standard b-y. Define any symbols you use.
- 4. (15 pts) All of the stars in Figure 2 gain their energy through nuclear reactions.
 a.(5 pts) Show that to penetrate the coulomb barrier the thermal temperature of a gas is given by

$$T = 2Z_1Z_2e^2/3kr$$

b. (5 pts) It is not clear in this expression what to use for r. Assume that the radius needed to penetrate the coulomb barrier is the de Broglie wavelength $\lambda = h/p$. Show that this allows T to then be expressed as

$$T = 4\mu Z_1^2 Z_2^2 e^4 / 3kh^2$$

c. (5 pts) In the Sun nuclear reactions take place at 10^7 K. Show that the temperature required for the helium flash to occur at the tip of the red giant branch is likely to be larger than 10^8 K.

- 5. (5 pts) Using the information in Figure 1 as a guide, discuss whether the scatter in b-y in Figure 2 (say at V=18) is due to observational error, or is their a significant unknown source causing the scatter in b-y?
- 6. (4 pts). How would the color-magnitude diagram seen in Figure 2 be changed for stars having V <16 if instead of V verses b-y this color magnitude diagram employed u verses u-y? Hint: Keep in mind that Figure 2 contains both cluster and field stars.)

For questions 7,8, and 9 you will use the figures on the attachment. The top figure is Figure 3 from the cume paper with some specific locations marked. The bottom figure shows the internal structure of a 1 solar mass star taken from Iben, 1967, ApJ 147, 624.

- 7. (7 pts) Examine the temperature, Luminosity, and Hydrogen profiles (labeled T, L, X_H) in the lower attached figure. What evolutionary state seen in Figure 3 does this structure correspond to? Explain your answer.
- 8. (15 pts total)

a. (10 pt) The number 1 in the attached top figure indicates the region populated by the RR Lyrae stars. They pulsate and obey a period-density relation. Using the adiabatic sound speed $v(r)_s = (\gamma P(r)/\rho)^{1/2}$ and the hydrostatic equation (with ρ unrealistically assumed to be constant), and approximating the pulsation period Π by the relation $\Pi \sim \int dr/v_s$ where the integration extends from r=0 to R, show that

$$\Pi = (3\pi/2G\pi\rho)^{1/2}$$

(hint $\int dr/(R^2 - r^2)^{1/2} = \pi/2$ when integrated form 0 to R)

- b. (5pts) Why do stars pulsate?
- 9. (15 pts total) To answer the following questions refer to the top attached figure. (A) (5 pts) Describe the inner structure of a star located a position 2
 - (B) (3 pts) What are stars at location 3 called?
 - (C) (4 pts) Assuming the star at location 4 is a cluster member, what is its likely evolutionary state?
 - (D) (3 pts) What is the name of the stars that occupy location 5

CCD uvbyHß PHOTOMETRY IN CLUSTERS. II. THE NEAREST GLOBULAR CLUSTER, NGC 6397

BARBARA J. ANTHONY-TWAROG¹ AND BRUCE A. TWAROG¹
Department of Physics and Astronomy, University of Kansas, Lawrence, KS 66045-2151; bjat@ukans.edu, twarog@ukans.edu

*Received 2000 June 26; accepted 2000 August 22

ABSTRACT

M22, M55, and M13, it is concluded that the globular cluster red giants do not follow the same c_1 versus b-y and m_1 versus b-y relations as the field giants, even if the cluster sample is restricted to CN-weak giants. Comparison of the cluster turnoff stars with field dwarfs of comparable [Fe/H] in the c_1 versus b-y diagram implies that, within the uncertainties, there is no difference in age between the two samples. From a handful of field dwarfs with comparable [Fe/H] and accurate parallaxes, the modulus of NGC 6397, $(V - M_V)_0$, is calculated to be 12.15. Comparison with isochrones of the appropriate [Fe/H] with $[\alpha/H] = +0.3$ results in an age of 12.0 ± 0.8 Gyr. The ultraviolet color-magnitude diagram of the cluster is examined and compared with earlier work.

Key words: globular clusters: individual (NGC 6397) — techniques: photometric

1. INTRODUCTION

The determination of the fundamental parameters of distance, metallicity, and age for clusters, open or globular, has been a focus of stellar populations studies for decades. Because of the critical role of interstellar reddening in this pursuit, the degree of success has been variable within both classes of cluster, as well as between classes. Open clusters can be found in relative abundance within a modest radius around the Sun, but their concentration toward the disk makes the more distant clusters difficult to identify and more likely to be heavily reddened. Globular clusters are rich enough to be easily identified and disentangled from the field both near and away from the plane, but the nearest clusters are more than 2 kpc away, and the nearest is within the Galactic plane. Because of their extreme age, small errors in reddening can lead to significant errors in the absolute cluster age (Anthony-Twarog & Twarog 1994), even while differential techniques provide strict limits on the relative age scale (see, e.g., Sarajedini, Chaboyer, & Demarque 1997).

To surmount the problems inherent in studying these crucial objects, virtually every photometric and spectroscopic avenue has been attempted. An approach that has been around for over a decade but only recently has started to emerge as a viable avenue for large-scale studies is the use of $uvbyH\beta$ CCD photometry. For open clusters, this system has long been in use with traditional photometers and

Fortunately, the situation has improved continually over the last decade. The $uvbyH\beta$ system is well defined for halo dwarfs, primarily as a result of the extensive work by Schuster & Nissen (1988, 1989a, 1989b). The original survey of Bond (1980) has been repeated and expanded by Twarog & Anthony-Twarog (1991) and Anthony-Twarog & Twarog (1994, 1998) to produce a significant sample of field halo giants. Mean relations for the giants have been used by Anthony-Twarog & Twarog (1994) to define both a metallicity calibration of the m_1 index and a method for reddening determination based upon the c_1 versus b-y

CCDs. The primary application was driven by the definition of the system for hotter dwarfs, which were within observational reach for a significant sample of nearby open clusters but difficult to attack in distant globular cluster main sequences. This was especially true for the redsensitive CCD chips common a few years ago, which made the important u filter (~3500 Å) difficult to observe with except for the brightest stars, and because of the narrow bandpass of the $H\beta$ filter. Though the brighter giants were within reach in both open and globular clusters, the uvby system was virtually undefined for cooler stars, with the exception of the pioneering work of Bond (1980) on metalpoor giants and a preliminary attempt for dwarfs by Olsen (1984). A further limitation to globular cluster work was the paucity, if not total absence, of potential standard stars within the clusters, required to set adequately the photometric zero point. The one advantage held by the globular over the open clusters was the richness of the sample; field star contamination was less significant and could be minimized using the metallicity-sensitive index, m_1 , to isolate field stars from cluster members in the more metal-poor clusters.

¹ Visiting Astronomer, Cerro Tololo Inter-American Observatory, National Optical Astronomy Observatories, operated by the Association of Universities for Research in Astronomy, Inc., under cooperative agreement with the National Science Foundation.

diagram. Applications of these techniques may be found in Twarog & Anthony-Twarog (1994, 1996a). Comparable approaches on slightly different systems have been promoted by Eggen (1984a, 1984b, 1990) and by Olsen (1993, 1995). Technically, the development of large-format, ultraviolet-sensitive CCDs has made the observational task of obtaining the necessary data less onerous.

This study is the second in a series of cluster analyses whose general focus is laid out in Anthony-Twarog & Twarog (2000, hereafter Paper I). Though the dominant sample of the larger program is open clusters, NGC 6397 was initially included because it was observable with a telescope of modest size, and our previous work pointed to the need for H β observations of this cluster to define reliably the cluster reddening. The progress in the area of intermediate-band CCD studies of globular clusters is readily illustrated by the sequence of papers starting with the first study of one small field of NGC 6397 by Anthony-Twarog (1987) on the uvby system, followed by a multiple set of small fields in only vby emphasizing the mainsequence structure and color-magnitude morphology (Anthony-Twarog, Twarog, & Suntzeff 1992), to the current investigation in which one large field is analyzed in all six filters of the uvbyH\$\beta\$ system. Other clusters studied in the uvb v system include ω Cen (Mukherjee, Anthony-Twarog, & Twarog 1992), M22 (Anthony-Twarog, Twarog, & Craig 1995), and NGC 6752 (Folgheraiter et al. 1995). Recent studies using only vby data include M55 and M22 (Richter, Hilker, & Richtler 1999) and ω Cen (Hughes & Wallerstein 2000). The only study involving a complete sample of uvbvHB photometry is a preliminary discussion of results in M13 by Grundahl, VandenBerg, & Andersen (1998)

The outline of the paper is as follows: § 2 details the observations, their reduction, and transformation to the standard system, § 3 delineates the procedure for isolating the probable cluster stars from the field, § 4 derives the fundamental cluster parameters from the probable members, § 5 discusses the implications of the photometry, and § 6 provides a summary of the conclusions.

2. OBSERVATIONS

2.1. Photoelectric Data

One of the more challenging aspects of CCD photometry, particularly with nontraditional intermediate-band systems. is the transformation of the instrumental indices and magnitudes to the standard system. Though cluster CCD frames may be calibrated using transformations derived from observations of standard stars taken on the same photometric night as the program frames, unlike classical photoelectric photometry, CCD observation of standard stars is often time-consuming and inefficient when attempted with a large-format chip. For globular clusters, the observed field invariably exhibits significantly greater problems with crowding, making the procedure for processing the frame distinctly different from that for a single bright standard observed in the field. The optimum procedure is to have a calibration defined by standard stars observed on the same night as the program cluster, but with internal secondary standards available in the cluster frames to provide a check on the slope and, especially, the zero point of the photometry.

With this in mind, photoelectric photometry on the uvbyCa system of a modest sample of brighter stars in NGC

6397 was obtained over a series of runs at Cerro Tololo Inter-American Observatory between 1990 and 1992. The data were collected within the context of a program to observe field halo giants using traditional photometers on the 1.0 m and 1.5 m telescopes; the data for NGC 6397 were obtained only with the 1.5 m telescope. A discussion of the reduction and standardization of the photometry is presented in detail in Anthony-Twarog & Twarog (1994) and will not be repeated here. The key points for the current investigation are that

1. The cluster photometry is on the same system as the field star data, i.e., the *uvby* system originally defined by

Bond (1980);

2. The metallicity and reddening relations used to estimate these key cluster parameters are defined by the same field giants, observed and reduced during the same runs as NGC 6397.

Thus, irrespective of questions about the absolute metallicity or reddening scale, one may obtain a very reliable differential estimate for the giants in NGC 6397 compared with the halo field stars.

The photoelectric observations for NGC 6397 are found in Table 1, where the first column lists the stellar identification on the systems of Woolley et al. (1961) and Alcaino (1977). The remaining columns are straightforward.

2.2. CCD Data: Observations and Processing

New photometric $uvbyH\beta$ data for NGC 6397 were obtained in 1997 July with the Cassegrain-focus CCD imager on the 0.9 m telescope at Cerro Tololo Inter-American Observatory. The field size for this 2048 \times 2048 Tektronix detector is 13.5 on a side at the f/13.5 focus of the 0.9 m telescope. Further details on the instrument and pre-liminary data processing steps are included in Paper I.

Our procedure begins with the processing of every frame using the ALLSTAR profile-fitting algorithms within the IRAF versions of the DAOPHOT packages. Each frame may yield instrumental magnitudes for thousands of stars, identified only by position. The instrumental magnitudes and associated errors for each frame are checked, and limits for inclusion in the composite average are defined based upon the error distribution with magnitude and the individual χ-values defining the quality of the fit of the pointspread function (PSF) to the stellar image. We employ software that collates instrumental magnitudes for stars in a common field by matching the stars' positions to some preset threshold, typically 1 pixel or less. As an intermediate stage, instrumental magnitudes for each star and from each frame of a similar color are grouped in a large array. The next step in the process is to determine and remove any systematic difference between the magnitude scale of one frame and another prior to construction of a weighted average magnitude for each star in each color. Unless a star has only one observation in a given color, the associated error for a magnitude is determined solely by frame-toframe comparisons.

The products of these software operations are magnitudes and indices for each star, internally precise and self-consistent to a high degree but not yet related to the standard system. A plot of the final standard errors of the mean for the V magnitudes and the various indices as a function of V is shown in Figure 1. That additional step requires either photoelectric measurements for some stars in the CCD field, a calibration for the night based on aper-

TABLE 1
PHOTOELECTRIC PHOTOMETRY IN NGC 6397

Identification	V	σ_V	by	σ_{b-y}	N_{yb}	m_1	σ _{m1}	c_1	σ_{c1}	N_{vu}
Alc 47	12.100		0.696		1	0.340		0.382		1
Alc 79	12.246		0.615	***	1	0.018	•••	0.524	•••	1
Alc 81	13.516	0.010	0.494	0.010	2	0.134	0.012	0.454	0.015	.2
Alc 93	12.687	0.023	0.649	0.008	2	0.089	0.010	0.402	0.011	.2
Alc 204	12,481	0.020	0.414	0.009	. 4	0.098	0.011	0.483	0.015	4
Alc 206	10.938	0.005	0.821	0.001	2	0.108	0.003	0.672	0.008	. 2
Alc 229	14.067		0.610		1	0.042		0.342	•••	1
Alc 302	10.401		0.921		1	0.229		0.689	•••	1
Alc 297	13.427		0.133	•••	1	0.062		1.102		1
Alc 305	11.682		0.721	•••	· 1	0.078		0.489	***	1
Alc 332	11.488		0.754		1	0.121		0.587	• • • •	1
Alc 366	10.715	•	0.851		1	0.170		0.668	***	- 1
Alc 390	12.350	•••	0.394		1	0.100	•••	0.474		. 1
ROB 25	12.202		0.682		1	0.090	•••	0.468	•	1
ROB 591	12.626		0.667		1	0.071	***	0.394	·:	1

ture magnitudes of standard stars, or a combination of the two.

2.3. Calibration to the Standard System: Hβ

Observations with H β filters were obtained on two nights, 1997 July 2 and 3, with the first of these two nights photometric. In all, nine H β w frames, with typical exposure times of 250 s, and 10 H β n frames, with exposure times from 900 to 1500 s, were obtained.

The basis for the $H\beta$ calibration employed for the IC 4651 data obtained on these nights was discussed in Paper I. Observations of stars in young open clusters helped to define the slope of the $H\beta$ calibration, while the intercept was determined with reference to 10 field standards and 14 cluster stars from IC 4651 observed on the one photometric night. We applied the same calibration strategy to the reduction of $H\beta$ indices in NGC 6397. Using the same criteria and apertures as were used for the field and cluster

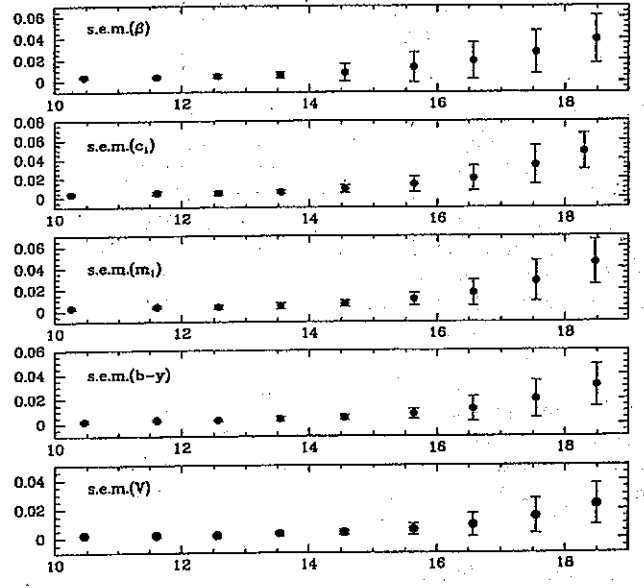


Fig. 1.—Standard errors of the mean for each index as a function of V

standard stars, aperture magnitudes were obtained for 26 relatively isolated stars in NGC 6397 for which CCD $H\beta$ indices were also available. The six $H\beta$ w and seven $H\beta$ n frames obtained on the photometric night were used for this purpose. The difference between CCD and aperture indices was determined from the 14 stars admitting the tightest determination of this "aperture correction"; even so, this correction introduces a modest uncertainty (± 0.006 s.e.m., standard error of the mean) to the zero point of the calibration equation, raising the estimate of the standard error of the mean of the calibration equation's zero point to ± 0.012 mag.

We compared our calibrated CCD HB indices with photoelectric values for seven stars measured by Ardeberg, Lindgren, & Nissen (1983, hereafter ALN) near the cluster turnoff. These are clearly very difficult photoelectric measurements, so it is easy to see how the dispersion of differences (photoelectric minus CCD) could be as large as ± 0.039 mag about a mean value of -0.012 mag. Since the standard error of the mean for this comparison is larger than the implied offset, we did not make any correction for this slight difference with respect to ALN's $H\beta$ photometry. It should also be noted that the H β indices of IC 4651, obtained during the same run and transformed using the same external calibration, exhibited an offset of only -0.002 ± 0.015 from a comparison with 14 stars with photoelectric photometry within that cluster; as with NGC 6397, the scatter originates almost exclusively with the photoelectric data.

2.4. Calibration to the Standard System: uvby

Two nights were dedicated to obtaining uvby frames in NGC 6397, with one night photometric. Ultimately, 10 frames in most colors, with 15 u frames, were obtained. Exposure times for the Strömgren bandpasses were typically 90-100 s for y, 200 s for b, 400 s for v, and 900-1500 s for u exposures. All of these frames were processed through ALLSTAR as described above; frames from the photometric night (six in each color) were additionally measured for aperture magnitudes in a manner identical to the measurement of magnitudes for the 10 field star standards.

Paper I described how this procedure hit a snag in the calibration of *uvby* indices for IC 4651 stars; a similar problem arose with NGC 6397. In canonical fashion, the

field stars were used to determine the slopes and intercepts of linear equations relating the standard values for each index to its instrumental equivalent, sometimes including a color term. Following the normal practice for photoelectric reductions, these linear solutions are broken at a color $b-y\sim0.4$; an additional distinction between dwarf and giant calibration lines is also common, especially for b-y, and indeed is the basis of subtle but important distinctions between subsets of this complex photometric system.

As acknowledged in Paper I, these approaches did not lead to a satisfactory calibration for IC 4651, so use was made of cluster photoelectric photometry to modify the zero points of the calibration equations. As the greatest adjustment was to the m_1 indices, for which the field standards were an admittedly poor match, this seemed a reasonable concession. Such should not be the case for the present application of the same calibration equations to the stars of NGC 6397, for which the field star standards should be an ideal match to at least the dwarfs.

Aperture measurements of about 20 stars were obtained using the *uvby* frames from the photometric night. All of these stars also have ALLSTAR-based indices, allowing for determination of the aperture corrections to the PSF-based instrumental indices. These corrections were determined with sufficient precision to add only ± 0.005 to the standard error of the mean for the zero points of the V and b-y calibration equations, with respective values of ± 0.011 and ± 0.020 for m_1 and c_1 . Applying the aperture corrections allows direct application of the linear calibration equations determined from the field star standards, with accompanying standard errors of the mean for the zero points of 0.005, 0.006, 0.013, and 0.020 mag for V, b-y, m_1 , and c_1 , respectively.

An assessment of how well this worked required an independent source of photometry, for which we appealed again to the photoelectric study by ALN. Seven dwarfs from their sample are also in the presently studied field of NGC 6397. The constructed differences in the sense photoelectric minus CCD with their standard errors of the mean are as follows: 0.017 ± 0.007 for V, -0.020 ± 0.003 for b-y, 0.048 ± 0.004 for m_1 , and 0.033 ± 0.005 for c_1 . If the photoelectric indices are taken to reflect more accurately the standard system, these offsets imply that our calibrated m_1 and c_1 indices are too large, reproducing the problem with respect to the m_1 values that was found for the IC 4651 standardization.

Our final solution to this recurring problem was to return to the field star standards with an eye to defining the form of the calibration from the field stars, while appealing to the internal standards to tie the zero points of the calibrations, effectively the same approach as used in Paper I. The forms of the calibration equations for m_1 and b-y were allowed to be quadratic, an option that also made it possible to smoothly transition between dwarfs and giants. The calibration equation for b-y contains terms equivalent to a slope 5% smaller than unity for the bluest stars near the blue horizontal branch, with a slope that exceeds unity for the reddest giant branch stars. The m_1 coefficients simulate a change in slope between m_1 and m_i from 1.05 to 1.15 for the reddest giants; the steepening slope effectively replaces a color term for the m_1 index. We did retain a linear calibration equation for c_1 , with a substantial color term adding $0.36(b-y)_i$ to the instrumental c_i index for stars redward and brighter than the cluster turnoff. It should be emphasized that a large color term is not unexpected given the inclusion of the u filter in c_1 when applied to red giants. We effectively predetermined which stars would be subjected to transformation equations appropriate for giant stars, as it appeared that the instrumental c_1 indices for the fainter stars might not provide sufficiently precise discrimination between dwarf and giant indices.

Once again, it is appropriate to construct comparisons with external sources of photometry to judge the reliability of our standardization equations. Seven dwarfs with photoelectric indices from ALN may be compared with the calibrated ALLSTAR-based photometry, as may the seven stars with photoelectric photometry discussed in the previous section and included in Table 1. The calculated differences and their standard errors of the mean, in the sense photoelectric minus CCD, for 14 photoelectric stars are -0.004 ± 0.011 for V, -0.014 ± 0.008 for b-y, 0.018 ± 0.008 for m_1 , and 0.010 ± 0.014 for c_1 . The final zero points were selected to eliminate any difference between the calibrated CCD indices and the photoelectric values for the seven evolved stars discussed in § 2.1 and included in Table 1. The standard errors of the mean for the differences for these seven stars alone are 0.011, 0.004, 0.007, and 0.006 for V, b-y, m_1 , and c_1 , respectively.

Graham & Doremus (1968) published some of the first Strömgren photometry in a globular cluster, concentrating on the bluer horizontal-branch stars. The blue horizontal-branch stars are readily identified by their large instrumental c_1 indices, though it is not clear which, if any, of our calibration schemes would be most appropriate to apply to them. By default, the blue horizontal-branch stars were treated with linear calibration equations with zero points adjusted to match the 22 stars in common with Graham & Doremus (1968). The standard errors of the mean for these instrumental comparisons are 0.005, 0.003, 0.005, and 0.010, respectively, for $V, b-y, m_1$, and c_1 .

A final summary of the uvby calibration and the system defined by the CCD data is as follows: For each of the three primary groups-giants, turnoff stars, and horizontalbranch stars—the form of the calibration relations was set using only stars with reliably determined photoelectric values. For the giants, these were the data of Table 1. For the dwarfs, the relations were set using only the field star and open cluster standards; for the horizontal-branch stars, the calibration was tied exclusively to the data of Graham & Doremus (1968). For the zero points, the giant photometry was tied exclusively to the data of Table 1, which is on the system of Anthony-Twarog & Twarog (1994, 1998) and Bond (1980); the uncertainty in the zero points for all the indices is ± 0.007 or less and is consistent with the errors in the photoelectric photometry alone. The zero points for the horizontal-branch photometry are set by the system of Graham & Doremus (1968) alone; as noted above, the uncertainty in the zero points is ± 0.010 or less for all the indices.

For the dwarfs, the zero point of the photometry is effectively set by the red giants, though the calibration curves have been defined to allow a smooth transition between the giants and the dwarfs. What photometric system is the dwarf/turnoff photometry on? Fortunately, at the same time the *uvby* data were obtained to set up the catalog of metal-poor red giant observations, a modest sample of dwarfs from the *uvby* catalog of metal-poor stars by Schuster & Nissen (1988) was also observed and transformed

using the calibration based upon the red giants. For b-y, the dwarfs were on the same system as the giants with a zero-point difference of less than 0.003 mag. For m_1 , there was a difference between the systems that was strongly dependent on m_1 with an offset near -0.03 mag, in the sense of the giant-based calibration minus the catalog m_1 , for solar-metallicity stars. However, for stars at the metallicity and color of the turnoff of NGC 6397, the difference in the zero points of the two systems is less than 0.002 mag. For c_1 , the red giant calibration produced an overall offset of +0.015 mag compared with the data in Schuster & Nissen (1988), though this discrepancy exhibited a much milder metallicity dependence than m_1 . At the abundance of NGC 6397, the red giant calibration produced c_1 indices too large by 0.011 mag at the color of the turnoff stars in NGC 6397.

The final photometry with self-explanatory column headings is given in Table 2. Stars appear in this table if they are brighter than V=18.0 and were measured on at least two y and b frames. About 65 stars have cross identifications

noted in the first column of the table. These identifications refer to numbering systems of Woolley et al. (1961; ROB), Alcaino (1977; Alc), Alcaino & Liller (1980; A&L), and Rubenstein & Bailyn (1996; R&B), and to the variable star survey by Kaluzny (1997; V).

3. CLUSTER MEMBERS: SAMPLE SELECTION

As discussed in § 1, the ultimate goal of this photometric program is to determine with the highest precision possible the fundamental cluster parameters of reddening, metallicity, and distance. Ideally, one would have proper-motion and radial velocity membership information that allowed the observer to isolate a sample minimally contaminated by field interlopers. Moreover, identification of binaries would permit the elimination of stars whose structure and evolution may have been altered by their proximity to other stars. In short, the cluster properties could be obtained from as pure and representative a sample as possible (see, e.g., Daniel et al. 1994; Nordström, Andersen, & Andersen 1997).

TABLE 2
CCD PHOTOMETRY IN NGC 6397

			CCD PHOTOMETRI IN INGC 0397															
X _{CCD}	Y _{CCD}	Ident.	V	b-y	m ₁	c ₁	β	$\sigma_{_{\hspace{1em}{V}}}$	σ_{by}	σ_{m1}	σ_{c1}	σ_{β}	N,	N _b	N,	N,	N _w	N,
1473.4	1878.9	·	9.922	0.862	0.756	0.394	2.537	0.002	0.002	0.004	0.004	0.003	6	7	7	9	6	9
1443.6	2021.8		9.925	1.060	0.325	0.750	2.516	0.002	0.002	0.002	0.003	0.005	6	8	3	8	4	8
561.1	463.1	4	10.228	0.989	0.265	0.747	2.520	0.001	0.002	0.003	0.004	0.004	6	6	7	9	4	7
828.3	1756.4		10.736	0.844	0.149	0.639	2.506	0.002	0.002	0.005	0.007	0.004	4	. 5	1	5	3	6
1122.6	1029.7	Alc 206	10.939	0.819	0.121	0.669	2.498	0.001	0.003	0.005	.0.005	0.005	4	5	6	6	4	4
1031.1	1857.8		10.979	0.813	0.142	0,624	2.506	0.001	0.003	0.005	0.006	0.004	8	5	1	6	4	6
624.5	1680.2	•••	11.014	0.819	.: 0.131 °	0.653	2.511	0.002	0.002	0.003	0.004	0.002	7	8	6	11	4	8
845.6	1685.1		11.096	0.793	0.117	0.609	2.513	0.001	0.002	0.003	0.004	0.003	7	7	• 4	12	4	10
365.1	1596.9	· · · ·	11.193	0.794	0.112	0.620	2.510	0.003	0.003	0.004	0.004	0.004	. 5	8 .	6	. 8	5	8
957.2	1921.1		11.209	0.788	0.098	0.615	2.506	0.002	0.002	0.004	0.006	0.005	7	8	4	6	4	9.
716.5	1985.2		11.404	0.760	0.080	0.547	2.509	0.003	0.003	0.004	0.005	0.007	5	7	5	10	4	5
931.0	1642.2		11.430	0.761	0.088	0.558	2.508	0.001	0.003	0.005	0.006	0.003	5	4	4	8	4	7
1508.5	2011.4	Alc 332	11.446	0.747	0.115	0.566	2.508	0.002	0.003	0.004	0.005	0.004	6	8	6	8	5	7
1089.6	1982.0		11.449	0.743	0.103	0.530	2.510	0.002	0.002	0.005	0.007	0.007	6	6	4	9	3	6
1554.6	1757.1	ROB 428	11.490	0.752	0.105	0.553	2.502	0.001	0.002	0.003	0.005	0.004	8	. 8	8	12	5	8
1016.0	367.0	•••	11.538	0.738	0.117	0.540	2.510	0.006	0.006	0.006	0.003	0.006	3	6	5	10	4	6
489.3	1660.7	•••	11.542	0.747	0.092	0.570	2.507	0.002	0.002	0.003	0.002	0.003	7	8	7	11	7	8
836.5	1677.0	• • • •	11.542	0.749	0.083	0.547	2.512	0.002	0.003	0.004	0.004	0.003	8	5	4	10	4.	õ
810.7	1902.5	*	11.700	0.734	0.075	0.554	2.497	0.002	0.003	0.005	0.006	0.005	6	5.	5	7	1	5
1019.2	1889.0		11.779	0.722	0.082	0.509	2.503	0.002	0.002	0.004	0.005	0.004	8	8	4	10	5	8
1260.9	1498.9		11.779	0.732	0.073	0.553	2.500	0.001	0.002	0.004	0.005	0.004	4	5	6	8	4	5
1113.7	1673.2		11.781	0.719	0.081	0.513	2.502	0.002	0.002	0.004	0.005	0.005	5	6	5	10	4	6
1116.2	1709.0	•••	11.818	0.678	0.041	0.533	2.509	0.002	0.005	0.007	0.005	0.005	5	3	7	11	3	6
1752.9	975.0	ROB 28	11.832	0.675	0.041	0,553	2.503	0.002	0.002	0.004	0.005	0.004	8	7	6	8	4	5
788.3	1886.0	***	11.852	0.671	0.038	0.537	2.516	0.002	0.003	0.004	0.004	0.004	. 7	8	7	10	4	8
890.5	1874.9	•••	11.905	0.724	0.069	0.533	2.505	0.001	0.002	0.003	0.004	0:005	7	9	7	10	. 3	7
1773.7	249.9	•••	11.940	0.418	0.123	0.356	2.579	0.002	0.003	0.004	0.005	0.004	6	8	5	6	5	5
1827.2	577.9		11.944	0.864	0.737	0.407	2.539	0.000	0.001	0.003	0.005	0.005	7	8	8	10	5	7
1167.3	1794.4	•••	11.980	0.699	0.074	0.510	2.506	0.002	0.003	0.009	0.012	0.004	4	2	2	8	4	7
729.6	1874.2	•••	11.981	0.657	0.029	0.537	2.521	0.002	0.003	0.005	0.005	0.003	. 7	8	4	10	5	8
1140.8	1918.3	•••	12.081	0.696	0.067	0.493	2.505	0.002	0.003	0.004	0.004	0.003	. ,	8	7	11	7	9.
273.0	1344.4	ROB 75	12.123	0.645	0.028	0.520	2.523	0.002	0.002	0.003	0.003	0.004	6	7	5	9	5	8
1770.5	1695.5	ROB 128	12.191	0.687	0.079	0.465	2.497	0.002	0.002	0.003	0.004	0.004	7	8	6	11	5	9
1901.4	1023.9	ROB 25	12.217	0.680	0.080	0.471	2.481	0.002	0.002	0.003	0.005	0.005	8	8	8	9	4	7
. 971.2	1856.8		12.225	0.697	0.063	0.508	2.511	0.002	0.002	0.010	0.003	0.005	7	6	2	10	5	5
1050.9	105.9	ROB 718	12.241	0.484	0.246	0.369	2.584	0.005	0.004	0.015	0.014	0.005	2	4	7	9	5	5
556.8	1281.3	Alc 390	12.344	0.393	0.240	0.489	2.661	0.003	0.003	0.003	0.004	0.003		7	5	-10	_	
213.0	1158.0		12.345		0.062	0.455	2.546	0.003	0.003	0.004	0.002		- 4		,-		4	9
528.4	1574.4	***	12.343	0.616	0.002	0.455	2.532	0.002	0.003			0.005	6	8	7	12	5	7
370.1	1342.8	•••	12.351	0.681	0.064	0.319	2.532	0.003	0.004	0.007	0.009	0.010	2	3	1	6	4	4
370.1	1342.0	•••	14.532	1,001	V.U04	U.461	Z.318	0.002	0.002	0.004	0.004	0.004	7	7	7	11	5	9

Note.—Table 2 is presented in its entirety in the electronic edition of the Astronomical Journal. A portion is shown here for guidance regarding its form and content.

For globular clusters, one can often sidestep these issues because of the paucity of binaries outside the cluster core and the high ratio of cluster members to field stars within the tidal radius: NGC 6397 is no exception. For the brighter giants, a mixture of membership information exists from spectroscopic studies that permits the elimination of interlopers via radial velocity data (e.g., Gebhardt et al. 1995). Attempts to identify binaries at the turnoff via photometric anomalies (Anthony-Twarog et al. 1992) have confirmed the deficiency of probable candidates outside the core of the cluster, though the fraction is not zero, in part because of the potential for optical binaries in the crowded cluster field. Given the variable quantity and quality of the data, we will adopt the pragmatic approach outlined and applied to IC 4651 in Paper I, optimizing what is more easily obtainable, an extensive array of very accurate magnitudes and colors. The ultimate product of the approach is a sample of stars that is composed purely of cluster members with photometric indices of high precision. As demonstrated in Paper I, the completeness of the sample is irrelevant; all that matters is that nonmember contamination of the sample be minimized. Keeping nonmembers out is more important than keeping members in.

Finally, the underlying principle that determines the success of the technique is that the cluster members are homogeneous in age and composition. For globular clusters, this assumption is not always valid. Photometrically, the effects of abundance variations on the *uvby*Ca system have been demonstrated using the two extreme examples found within the globular cluster system, ω Cen (Mukherjee et al. 1992; Hughes & Wallerstein 2000) and M22 (Anthony-Twarog et al. 1995; Richter et al. 1999). Moreover, individual stars that have undergone significant mixing leading to an alteration in the surface abundances of CNO may exhibit anomalous indices relative to the mean for the halo giants of comparable [Fe/H] (Bond 1980; Anthony-Twarog & Twarog 1994). To date, there is no evidence for a significant spread in [Fe/H] among the stars in NGC 6397.

3.1. Thinning the Herd: The Color-Magnitude and Color-Color Diagrams for Red Giants

As our starting point, we present in Figure 2 the color-magnitude diagram (CMD) for NGC 6397, using b-y as the temperature index. The sample has been restricted to include only stars with at least two observations each in b

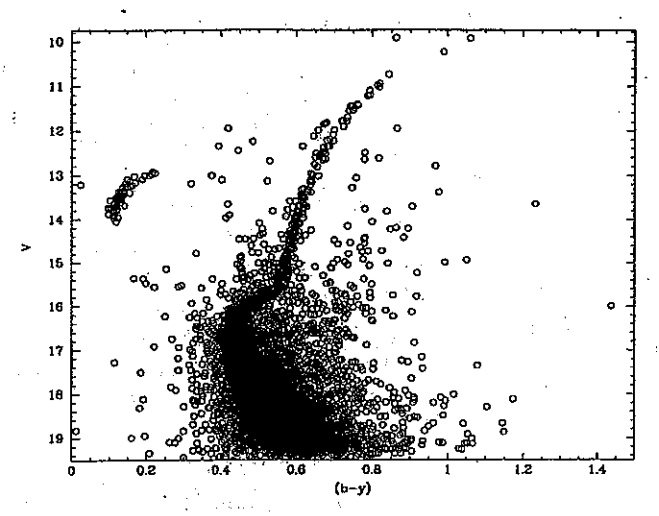


Fig. 2.—CMD for all stars with at least two observations each in b and v.

and y. The primary features of the CMD as delineated in Anthony-Twarog (1987) and Anthony-Twarog et al. (1992) remain unchanged, though the diagram is significantly richer because of the larger field of the CCD. It is obvious that the CMD is dominated by cluster members, though a nonnegligible scatter of stars does exist away from the mean cluster relations.

The high accuracy of the photometry demonstrated in Figure 1 allows us to make a second cut to reduce the sample further; only giants with a standard error of the mean in b-y of ≤ 0.010 will be analyzed (as discussed in § 3.2, for the turnoff we will soften this cut to 0.015 mag). The CMD resulting from the more restrictive cut is shown in Figure 3. The expanded scale, coupled with the removal of stars with larger photometric errors, provides more insight into the CMD structure. Most of the subgiant and giant stars remain, but the turnoff region becomes less populated with increasing V. However, the scatter exhibited in the complete sample of Figure 2 has been dramatically reduced, and the location of the primary sequence at the turnoff is beautifully defined.

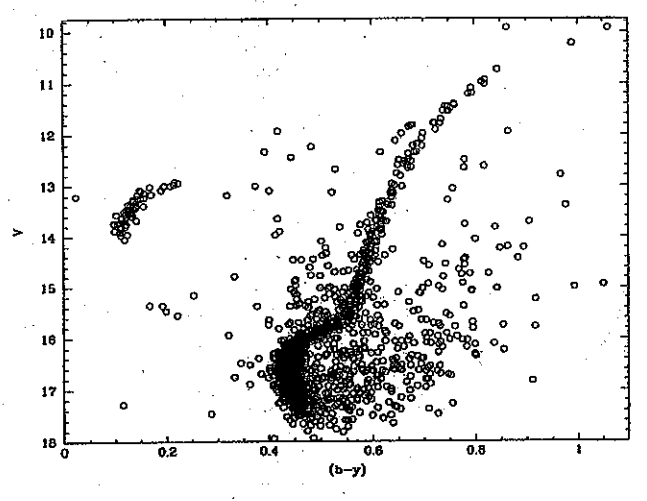


Fig. 3.—Same as Fig. 2, but with the additional restriction that the standard error of the mean in b-y be ≤ 0.010 .

Attach ment.

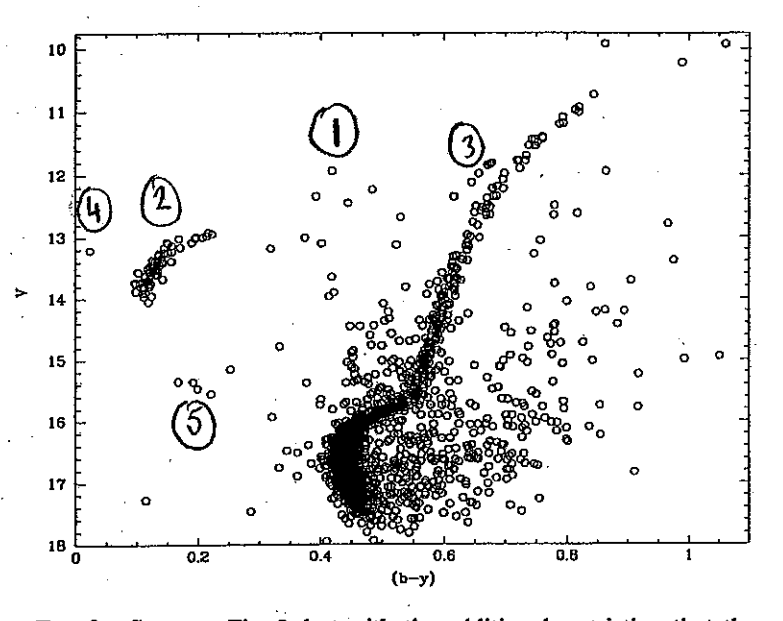


Fig. 3.—Same as Fig. 2, but with the additional restriction that the standard error of the mean in b-y be ≤ 0.010 .

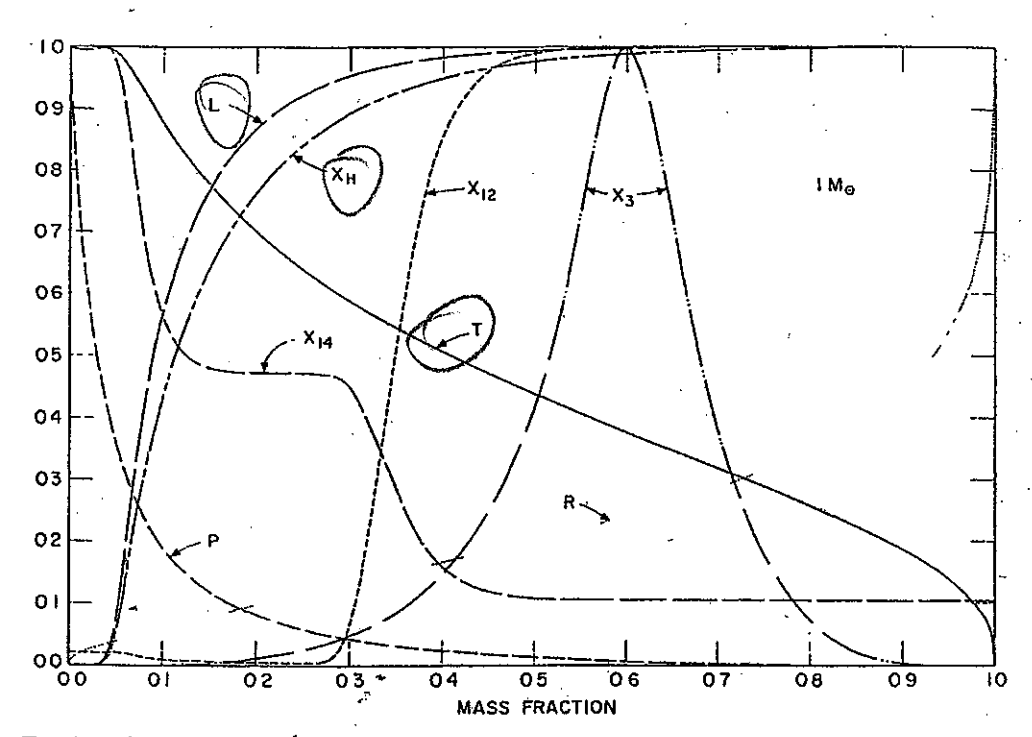


Fig. 9.—The variation with mass fraction, for a 1 $M\odot$ star, of state and composition variables when $t=9.20150\times10^9$ yr. Variables have the same significance and units as in Fig. 8 In addition, pressure P is given in units of 10^{17} dyne/cm². Scale limits correspond to $0.0 \le P \le 13$ 146, $0.0 \le T \le 19.097$, $0.0 \le L \le 2.1283$, $0.0 \le R \le 1.2681$, $0.0 \le X_{\rm H} \le 0.708$, $0.0 \le X_{\rm S} \le 5.15\times10^{-3}$, $0.0 \le X_{\rm H} \le 3.15\times10^{-3}$, and $0.0 \le X_{\rm H} \le 1.15\times10^{-3}$. Stellar radius is $R_{\rm S}=1.3526~R\odot$, and central density (not shown) is $1026.0~{\rm gm/cm^3}$.

answers

- 3 1. a why HB refer to the felters used in Strompren photometry

 6-3500 A v-4100 A, b-4700 A y = 5550 A, HB = 2 letters centered on HB, or of

 which is wide, other is married.

 3 b C, m. C, = surface granty index = (u-v)-(v-b)

 M = metalicity index = (v-b)-(b-y)
 - 3 c standard error of the mean std error = or, std error of mean : of
 - d instrumental magnetude = magnetude corrected for atmospheric absorption aperture is a magnetude more and an CCD image with specific aperture.

 Standard "= magnetude of a refer in a pre-defined phometric system
 - 3 & PSF Point spread function describes the stellar propile on a CCD. Chip
 - 2. a. HB measurements can be obtained on a non-photometric my to and ntell he wreful since they envolve the vatio of 2 measured Plunes at the same effective wavelength Measurement must be taken soon after each other for the described cancellations to be roled
 - In obtained under different sty conditions. A possible work-around is to use standard on the same CCD images as your target Nais. The hope here is that the stars have been semilarly affected
 - e. If one desired to determine the charter metabolity, reddening, distance it is not necessary to measure every star This generatives are the same for all go stars.
 - 3. One can either do form b-y from $b=b_0+k_bX$, $y=y_0+l_yX$ or $(b-y)=(b-y)_0+k_byX$. To then Transform These magnifiedes ento the standard system one determines litting constants from a relation like

(6-8) std = A(b-4)0+ B

In this paper The authors were concerned that higher order terms my ht he necessary to make this transformation.

y We are asked to compute a thermal temperature. This leads us to the approximation that the particles must have a temperature of

or
$$T = \frac{2}{3} \frac{2}{3} \frac{2}{kr} e^{2}$$
 (1)

The question ask one to publitute I for r.

$$\lambda = \frac{h}{P}$$

arrange that the lunate energy in the collesion must be sufficient to precious the collision

this is almost

This stell leave us with an unknown or, no wo

$$\frac{1}{2} M V^2 = \frac{P^2}{2M}$$
 So

$$2.\frac{2}{1}e^{2} = \frac{p^{2}}{2m} = \left(\frac{1}{2}\right)^{2}$$

$$\chi = \frac{h^2}{2m^2 l^2 e^2}$$

Gamy back to 1

For the Sun T = 107 k (5000). For the helium plank 2, 3, 2, 72, 12 + 4.4 ~ 2

Figure 5.e.m (b-y) at V=18 is a 0.03. The spread in Figure 2 about nome mean line looks to be about 0.5 The spread is ±35 about the mean arruning each mean in Figure 1 represents 4-9 pts

Expected spread = 0.03 × 2.5 × 6 ~ 0.45 (Close enough)

6 The answer to this question is provided later in the paper as Figure 11

The low metal abundance of the cluster compared to the field causes those two populations to become less consendent. The cluster stars are shifted to the blue (lower u-y) relative to the field.

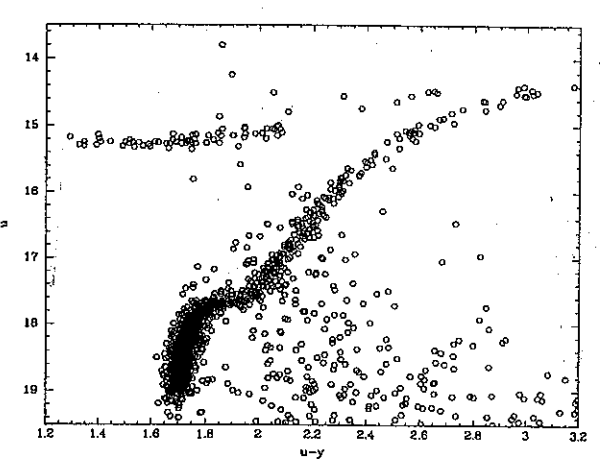


Fig. 11.—The u vs. u-y diagram for a restricted sample of stars with small errors in u

7 a) The T profile is flat over the inner ~ 5 h of the Nais radius = isothermal core!

b) The core is not contributing to L which rises quickly at a mass fraction £ 0.08-011

The onegy is being created in a contined envelop

9) There is no Hydrogen within the core

=> shell source > location just beyond the cluster turnoff.

8 Start with
$$y(r) = (8P)^2$$
 and the hydrostate equation
$$\frac{dP}{dr} = -G \frac{m_r P}{r^2}$$

One want P in terms of P

$$\int_{r}^{R} d\rho = -\int_{r}^{R} G \frac{m_{r} \rho}{r^{2}} dr = \int_{r}^{R} -G(\frac{4}{3} \pi r^{3} \rho) \rho dr$$

$$= -\frac{4}{3} G \pi \rho^{2} \int_{r}^{R} r dr$$

$$\int_{r}^{R} G \pi \rho^{2} \int_{r}^{R} r dr$$

$$\pi = 2 \int_{6}^{R} \frac{dr}{v_s} = 2 \int_{6}^{R} \frac{dr}{\sqrt{\frac{2}{3}\pi G \rho^{\gamma}(R^2 - r^2)}}$$

6. Pulsation is due to the presence of an opacity source that increases with T. This causes a build in prorraw as the star contracts When the pressure is released the New arenshosti calleposes aga v proceso repeate

9 (a) Location corresponds to a HB war = core helium burning + H burning shell

- asymptotic branch stars
- (c) Planetary mebula nucleus (?? enteresting bocation)
- (d) Blue straggless would occupy this region
- dropped (e) It most likely contains was they are too faint to be visible in this m-M=12.2

M ~ 10

m = 22!

Attach ment.

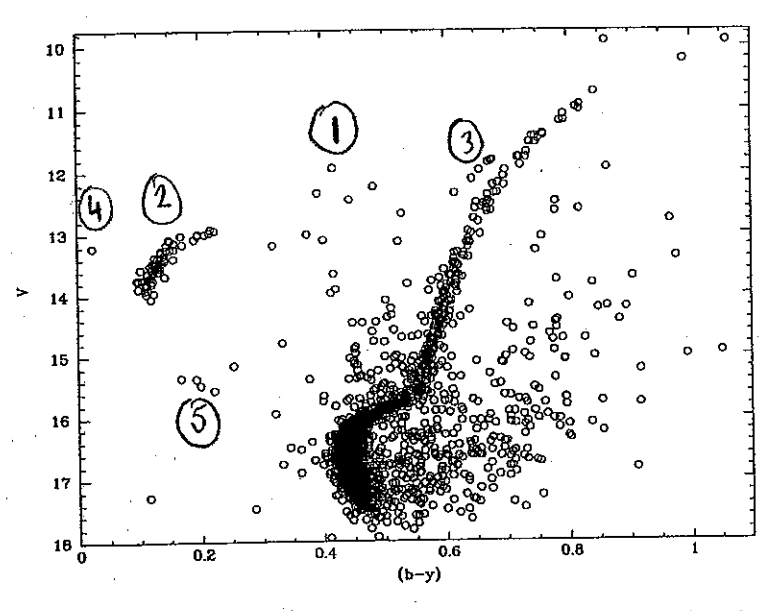


Fig. 3.—Same as Fig. 2, but with the additional restriction that the standard error of the mean in b-y be ≤ 0.010 .

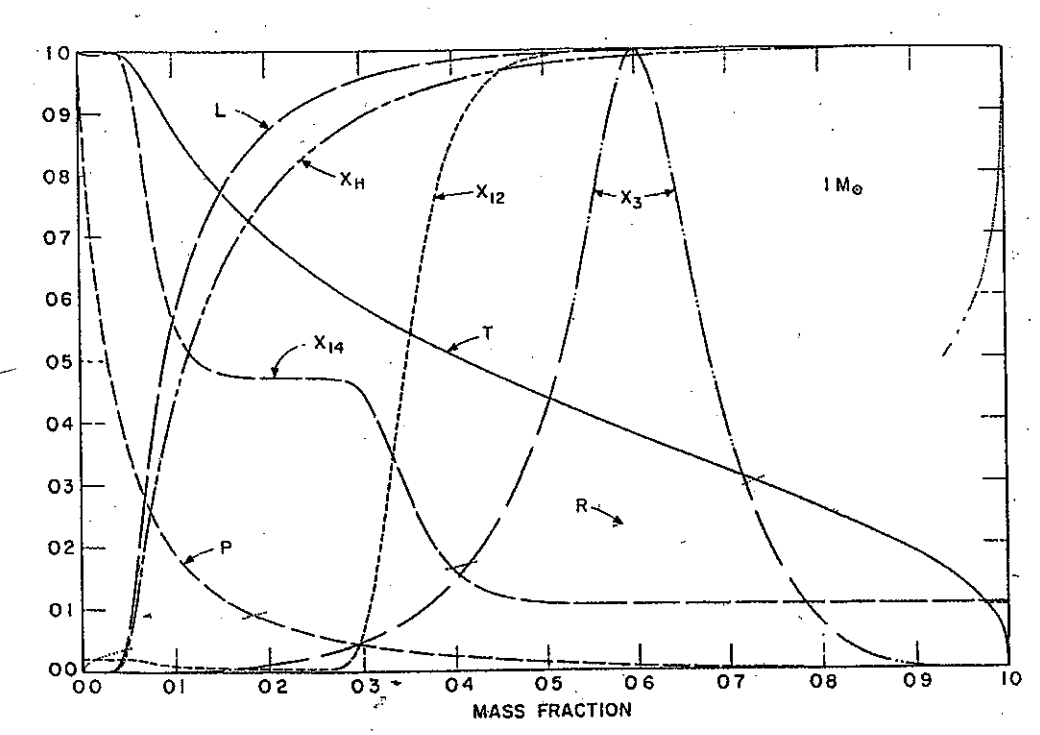


Fig. 9.—The variation with mass fraction, for a 1 $M\odot$ star, of state and composition variables when $t=9.20150\times 10^9$ yr. Variables have the same significance and units as in Fig. 8 In addition, pressure P is given in units of 10^{17} dyne/cm². Scale limits correspond to $0.0 \le P \le 13$ 146, $0.0 \le T \le 19.097$, $0.0 \le L \le 2.1283$, $0.0 \le R \le 1.2681$, $0.0 \le X_{\rm H} \le 0.708$, $0.0 \le X_4 \le 5.15 \times 10^{-4}$, $0.0 \le X_{12} \le 3.61 \times 10^{-4}$, and $0.0 \le X_{14} \le 1.15 \times 10^{-2}$. Stellar radius is $R_* = 1.3526$ $R\odot$, and central density (not shown) is 1026.0 gm/cm².